TNF-α blockade reverses Stevens-Johnson syndrome/toxic epidermal necrolysis through the RORγt/Foxp3-mediated restoration of T helper 17/regulatory T cell balance

ZHAO MA[1], WEI ZHANG[2], SAI-FEI XI[1], TING-TING SHI[1] and XIN-CHANG XU[1]

[1]Department of Pharmacy, Hangzhou Third People's Hospital, Hangzhou Third Hospital Affiliated to Zhejiang Chinese Medical University, Hangzhou, Zhejiang 310009, P.R. China; [2]Department of Chemical Drug Inspection, Hangzhou Institute of Food and Drug Inspection and Research (Hangzhou Center For Adverse Reaction Monitoring of Drugs and Medical Devices), Hangzhou, Zhejiang 310009, P.R. China

Received December 4, 2025; Accepted March 13, 2026

DOI: 10.3892/etm.2026.13159

Abstract. Within the present study, the aim was to examine how the expression of retinoic acid-related orphan receptor γ-t (RORγt) and Foxp3 influences the balance between T helper 17 (Th17) cells and regulatory T cells (Tregs) in a mouse model of Stevens-Johnson syndrome/toxic epidermal necrolysis (SJS/TEN) and to determine the association of this mechanism with the therapeutic response to a TNF-α blockade. A murine SJS/TEN model was induced and animals were assigned to three groups: Disease model, TNF-α inhibitor treatment and healthy control. The analytical methods conducted included histopathology (H&E and toluidine blue staining), measurement of serum cytokines using ELISA, flow cytometric quantification of Th17 and Treg frequencies in peripheral blood, immunohistochemical (IHC) evaluation and reverse transcription-quantitative PCR (RT-qPCR) analysis of RORγt and Foxp3 expression in isolated $CD3^+$ T lymphocytes. Mice in the model group displayed characteristic histopathological features, including widespread epidermal necrosis, dense dermal inflammatory infiltration and increased mast cell counts. Serum concentrations of IL-17 and IL-23 were elevated. Immune profiling demonstrated a higher frequency of Th17 cells, a lower frequency of Tregs and a consequently increased Th17/Treg ratio. Both IHC and RT-qPCR data indicated marked upregulation of RORγt and downregulation of Foxp3 at both protein and transcriptional levels. Treatment with a TNF-α inhibitor reversed these changes, resulting in ameliorated skin pathology, normalized Th17/Treg balance, reduced RORγt and restored Foxp3 expression. The degree of Foxp3 restoration and Th17/Treg rebalancing were positively correlated with a clinical improvement in skin lesions. Overall, disruption of Th17/Treg equilibrium, driven by dysregulation of the RORγt/Foxp3 axis within $CD3^+$ T cells, was found to be a key mechanism in SJS/TEN pathogenesis. TNF-α blockade exerts its therapeutic effect by transcriptionally reprogramming T cells, directly suppressing the expression of RORγt while promoting the expression of Foxp3. This bidirectional regulation corrects the Th17/Treg imbalance. These findings demonstrate the important immunomodulatory action of TNF-α inhibition and offer preclinical support for its use in SJS/TEN, while suggesting potential biomarkers for monitoring treatment efficacy.

Introduction

Stevens-Johnson syndrome (SJS) and toxic epidermal necrolysis (TEN) are severe, life-threatening cutaneous adverse reactions, most commonly triggered by medications such as antibiotics, anticonvulsants and NSAIDs, and characterized by extensive epidermal necrosis and detachment (1-3). Despite its low incidence (1-2 cases per million annually worldwide) (4), SJS/TEN remains a life-threatening condition with mortality rates ranging from 20 to 50%, primarily due to secondary infections, electrolyte imbalance and multiple organ failure (5). A recent nationwide analysis of 2,416 patients in the USA confirmed that SJS/TEN is associated with significantly increased risks of pneumonia, sepsis and respiratory failure requiring intubation, underscoring the substantial disease burden even in modern healthcare settings (6). Supportive care, systemic corticosteroids and intravenous immunoglobulin (IVIG) constitute the main methods of treatment; however, therapeutic efficacy varies markedly among patients and their use remains controversial (7-10). Corticosteroids broadly suppress inflammation but carry notable risks of infection, impaired wound healing and gastrointestinal bleeding, with no consensus on optimal dosing or timing having been reached (7,9). IVIG, while potentially beneficial, has yielded conflicting results across studies, primarily due to heterogeneity in patient selection, dosage

Correspondence to: Dr Xin-Chang Xu, Department of Pharmacy, Hangzhou Third People's Hospital, Hangzhou Third Hospital Affiliated to Zhejiang Chinese Medical University, 38 West Lake Avenue, Hangzhou, Zhejiang 310009, P.R. China
E-mail: xxinchang@163.com

Key words: Stevens-Johnson syndrome/toxic epidermal necrolysis, T helper 17/regulatory T cell, retinoic acid-related orphan receptor γ-t, Foxp3, TNF-α inhibitor, immunomagnetic bead sorting

regimens and disease severity (7,8). These therapeutic uncertainties and the absence of targeted interventions stem largely from an incomplete understanding of SJS/TEN pathogenesis, highlighting the need for mechanism-based approaches such as TNF-α blockades.

Accumulating evidence has suggested that SJS/TEN is initiated by a drug-specific immune response, whereby T cell-mediated cytotoxicity serves an important role in keratinocyte apoptosis (11-13). The balance between $CD4^+$ T cell subsets is key in immune homeostasis. T helper 17 (Th17) cells, defined by the master transcription factor retinoic acid-related orphan receptor γ-t (RORγt), drive inflammation through secretion of IL-17 and related pro-inflammatory cytokines, including IL-17A, IL-17F, IL-21 and IL-22 (14-16). By contrast, regulatory T cells (Tregs), characterized by expression of the transcription factor Foxp3, maintain immune tolerance and suppress excessive immune activation (17,18). An imbalance of the Th17/Treg ratio has been implicated in a number of autoimmune and inflammatory diseases, including rheumatoid arthritis, inflammatory bowel disease, multiple sclerosis and psoriasis (19-21). Clinical studies have reported increased Th17 cell frequencies and/or impaired Treg function in the peripheral blood and skin lesions of patients with SJS/TEN (22-24), suggesting that immune dysregulation may contribute to disease pathogenesis. Despite this, the precise role of Th17/Treg imbalances and the underlying regulatory mechanisms involving RORγt and Foxp3 expression remain to be systematically elucidated in a controlled experimental setting.

TNF-α serves as a key inflammatory mediator in SJS/TEN. Elevated TNF-α levels have been detected in patient serum and skin lesions and are associated with disease severity (25-27). Accordingly, TNF-α inhibitors such as etanercept and infliximab have emerged as promising alternatives in severe SJS/TEN cases, with numerous studies having reported favorable outcomes and potentially improved safety profiles compared with high-dose corticosteroids (3,28,29). However, treatment responses appear to be inconsistent, and whether the therapeutic effect involves transcriptional regulation of RORγt and Foxp3 expression to restore Th17/Treg balance remains unclear. Elucidating the effects of TNF-α blockade on Th17/Treg equilibrium and their key transcriptional regulators is important in understanding its therapeutic efficacy, predicting treatment response and developing optimized, evidence-based treatment algorithms.

Therefore, the present study aimed to establish a reliable SJS/TEN mouse model to investigate the following: i) Whether disease progression involves Th17/Treg imbalance and altered RORγt/Foxp3 expression; ii) the correlation between this immunologic imbalance and tissue damage/systemic inflammation; and iii) whether the therapeutic effect of TNF-α blockade is mediated through correction of this imbalance. The present research provided experimental evidence for the immunopathogenesis of SJS/TEN and a mechanistic rationale for the clinical application of TNF-α inhibitors as a targeted therapeutic strategy.

Materials and methods

Experimental animals and SJS/TEN induction. A total of 24 male BALB/c mice (6-8 weeks old; body weight, 20-25 g) were obtained from Hangzhou Hangsi Biotechnology Co., Ltd. [license no. SCXK(ZHE)2022-0005; animal qualification certificate no. 20250407Abzz01009990022]. The animals were maintained at Deruikang Biotechnology (Zhejiang) Co., Ltd. [license no. SYXK(ZHE)2023-0002] under standard conditions (22±2˚C; 60-80% humidity; 12-h light/dark cycle) with *ad libitum* access to food and water. The SJS/TEN-like model was established through cutaneous sensitization and challenge with trichloroethylene (TCE) as previously described (11), with the following modifications: i) The sensitization dose was reduced from 100 to 50% TCE to minimize systemic toxicity; ii) the challenge frequency was increased from a single application to two applications on days 17 and 19 to enhance skin lesion severity; and iii) the challenge concentration was adjusted from 50 to 30% TCE to balance efficacy and tolerability. Briefly, mice received an initial intradermal injection (100 µl) containing equal volumes of 50% TCE in olive oil and Complete Freund's Adjuvant. Subsequent sensitization was performed on days 4, 7 and 10 by topical application of 100 µl 50% TCE to shaved dorsal skin, covered with filter paper (1x1 cm) and secured with hypoallergenic tape for 24 h. Challenge phases were conducted on days 17 and 19 using 100 µl 30% TCE applied similarly. All experiments were repeated three times independently.

Study groups and drug administration. Animals were randomly assigned to four experimental groups (n=6/group): i) Vehicle control (NC), receiving olive oil instead of TCE throughout the procedure; ii) TCE model (M); iii) positive control (PC), administered methylprednisolone (4 mg/kg through intraperitoneal injection) 24 h before each challenge (days 16 and 18); and iv) TNF-α antagonist treatment group (T), administered infliximab (1 mg/kg through intraperitoneal injection; MedChemExpress) 24 h before the challenges on days 16 and 18. Drug doses were selected based on a previous study (24). All groups except NC underwent identical TCE exposure.

Clinical evaluation of skin reactions. Cutaneous responses were evaluated 24 h post-final challenge by two independent blinded investigators using a standardized scoring system (30,31): 0, no visible reaction; 1, scattered mild erythema; 2, moderate diffuse erythema with slight edema; or 3, severe erythema with pronounced swelling. In cases of disagreement, the final score was determined by consensus after discussion between the two investigators. Animals displaying scores ≥1 were considered sensitization-positive (TCE^+), while scores ≥3 were classified as meeting SJS/TEN-like criteria.

Tissue and blood sample preparation. Following anesthesia with 2% isoflurane for induction and 1.5-2% isoflurane for maintenance, mice were euthanized through cervical dislocation 24 h after the final challenge. No animals reached the pre-determined humane endpoints (including ≥20% body weight loss, severe lethargy or respiratory distress) prior to the scheduled endpoint. A total of ~100 µl blood was collected through retro-orbital puncture from each animal. Serum was obtained by centrifugation at 3,000 x g for 15 min at 4˚C and stored at -80˚C. Dorsal skin specimens (1x1 cm) were divided, with one segment being fixed in 4% paraformaldehyde

(in 0.1 M phosphate buffer, pH 7.4) at 4˚C for 24 h for histological processing, and another being flash-frozen in liquid nitrogen and stored at -80˚C for molecular analyses (32).

Histopathological and immunohistochemistry (IHC) examinations. Paraffin-embedded skin sections (5 μm) were processed for H&E staining. Briefly, sections were stained with hematoxylin for 5 min at room temperature, rinsed under running tap water for 10 min, counterstained with eosin for 2 min at room temperature, and then dehydrated using graded alcohols and xylene before mounting. Five random microscopic fields (magnification, x200) per section were analyzed for epidermal necrosis, dermal edema and inflammatory cell infiltration using an Olympus BX53 light microscope (Olympus Corporation). Mast cell quantification was performed using toluidine blue staining (33), with sections stained in 0.5% toluidine blue solution for 20-30 min at room temperature. All positively stained cells were counted in five non-overlapping high-power fields (magnification, x400). For IHC, sections underwent antigen retrieval in citrate buffer (pH 6.0) by heating at 95-100˚C for 20 min in a water bath, followed by cooling at room temperature for 30 min. Sections were then washed three times with phosphate-buffered saline (PBS, pH 7.4) for 5 min each, followed by overnight incubation (16-18 h) at 4˚C with the primary antibodies: Anti-RORγt (1:200; cat. no. ab207082; Abcam) and anti-Foxp3 (1:150; cat. no. 12653S; Cell Signaling Technology, Inc.). Endogenous peroxidase activity was blocked with 3% H_2O_2 in PBS for 10 min at room temperature. Sections were then incubated with HRP-conjugated secondary antibodies (goat anti-mouse IgG; 1:500; cat. no. RGAM001; Proteintech Group, Inc.; and goat anti-rabbit IgG; 1:500; cat. no. GAR0072; MultiSciences Biotech) for 1 h at room temperature. Visualization was performed using 3,3'-diaminobenzidine as the chromogen (34). The number of positive cells per high-power field (magnification, x400) was counted in five random fields.

Serum cytokine profiling. Commercial ELISA kits (Shanghai Enzyme-linked Biotechnology Co., Ltd.) were employed according to manufacturers' protocols to quantify circulating levels of IL-17, IL-23, IL-10 and TGF-β1. The ELISA kit cat. nos. were as follows: IL-17 (cat. no. ml-063129), IL-23 (cat. no. ml-063140), IL-10 (ml-037873) and TGF-β1 (cat. no. ml-002115). The detection ranges were 15.6-500 pg/ml for IL-17, 7.8-250 pg/ml for IL-23, 31.2-1,000 pg/ml for IL-10 and 62.5-4,000 pg/ml for TGF-β1. The limits of detection were <9.4, <4.7, <18.8 and <37.5 pg/ml, respectively. The intra-assay coefficients of variation (CV) were <9% and inter-assay CV were <11% for all kits, as certified by the manufacturer. **A** standard volume of 50 μl serum supernatant per sample was used for each assay. All samples were run in duplicate. Absorbance was measured at 450 nm using a microplate reader (BioTek; Agilent Biotechnologies).

Flow cytometric immunophenotyping. Peripheral blood mononuclear cells (PBMCs) were isolated from ~100 μl whole blood using Ficoll-Paque PLUS density gradient centrifugation (cat. no. 17-1440-02; Cytiva) (32). Furthermore, ~$1x10^6$ cells per sample were used for staining. For Th17 cell identification, cells were stimulated with phorbol 12-myristate 13-acetate (50 ng/ml) and ionomycin (1 μg/ml) in the presence of brefeldin A (10 μg/ml) for 5 h. Following stimulation, cells were fixed and permeabilized using the BD Cytofix/Cytoperm™ Kit (cat. no. 554714; BD Biosciences) according to the manufacturer's instructions. Cells were then stained with anti-CD4-FITC (clone RM4-4, 0.125 μg/test; cat. no. 11-0043-82; Thermo Fisher Scientific, Inc.) and anti-IL-17A-PE (clone 9L713, 10 μl/test; cat. no. TMAY-03535P; TargetMol) for 30 min at 4˚C in the dark (35). Tregs were identified using anti-CD4-FITC (clone RM4-4; cat. no. 11-0043-82; Invitrogen; Thermo Fisher Scientific, Inc.), anti-CD25-APC (clone PC61.5; cat. no. 17-0251-82; Invitrogen; Thermo Fisher Scientific, Inc.) and anti-Foxp3-PE (clone PCH101; cat. no. 12-4771-82; Invitrogen; Thermo Fisher Scientific, Inc.) antibodies using the Foxp3/Transcription Factor Staining Buffer Se (cat. no. 00-5523-00; eBioscience™; Thermo Fisher Scientific, Inc.). All antibodies were used at a 1:50 dilution following lot-specific titration optimization. Compensation was performed using the LongCyte™ flow cytometer (Beijing Cenglang Biotechnology Co., Ltd.) with automated software based on single-color controls. Furthermore, ≥10,000 events in the lymphocyte gate were acquired using a BD FACSCelesta™ flow cytometer (BD Biosciences). Th17/Treg ratios were calculated from CD4+ T cell subsets. All flow cytometry experiments were repeated three times independently. Data were analyzed using FlowJo™ software (v10.10; BD Biosciences).

$CD3^+$ T cell isolation and purification assessment. $CD3^+$ T lymphocytes were positively selected from PBMCs using the EasySep Mouse CD3 Positive Selection Kit II (Miltenyi Biotec, Inc.) following the manufacturer's protocol. Typically, $5x10^6$ PBMCs yielded 2-$3x10^6$ $CD3^+$ cells. Purity verification was performed through flow cytometric analysis using anti-CD3ε-APC antibody staining (clone 145-2C11; cat. no. 130-119-807; Miltenyi Biotec GmbH) for 30 min at 4˚C in the dark; only preparations >95% purity (determined by analysis of 5,000 events) were utilized for subsequent experiments.

Gene expression analysis by reverse transcription-quantitative PCR (RT-qPCR). Total RNA was extracted from ~$1x10^6$ purified $CD3^+$ T cells using the FastPure® Cell/Tissue Total RNA Isolation Kit V2 (cat. no. RC112-01; Nanjing Vazyme Biotech Co., Ltd.) according to the manufacturer's instructions. RNA concentration and purity were determined by NanoDrop spectrophotometry (A260/A280 ratio >1.8; Thermo Fisher Scientific, Inc.). After quality verification, 1 μg RNA was reverse-transcribed into cDNA using the PrimeScript™ RT Reagent Kit with gDNA Eraser (cat. no. RR047A; Takara Bio, Inc.) at 37˚C for 15 min, following the manufacturer's protocol. cDNA synthesis efficiency was ≥90% and genomic DNA removal efficiency was >99% as verified by no-RT controls. qPCR was performed using TB Green Premix Ex Taq II (Takara Bio, Inc.) in a 20 μl reaction volume containing 2 μl cDNA template. The dynamic range was 7 orders of magnitude and PCR efficiency was 95-105% (determined by a standard curve slope of -3.3 to -3.5). Reactions were run on an Applied Biosystems 7500 Real-Time PCR System (Applied Biosystems; Thermo Fisher Scientific, Inc.) under the following conditions: 95˚C for 30 sec, then 40 cycles of 95˚C for 5 sec and 60˚C for 30 sec. Melting curve analysis demonstrated primer

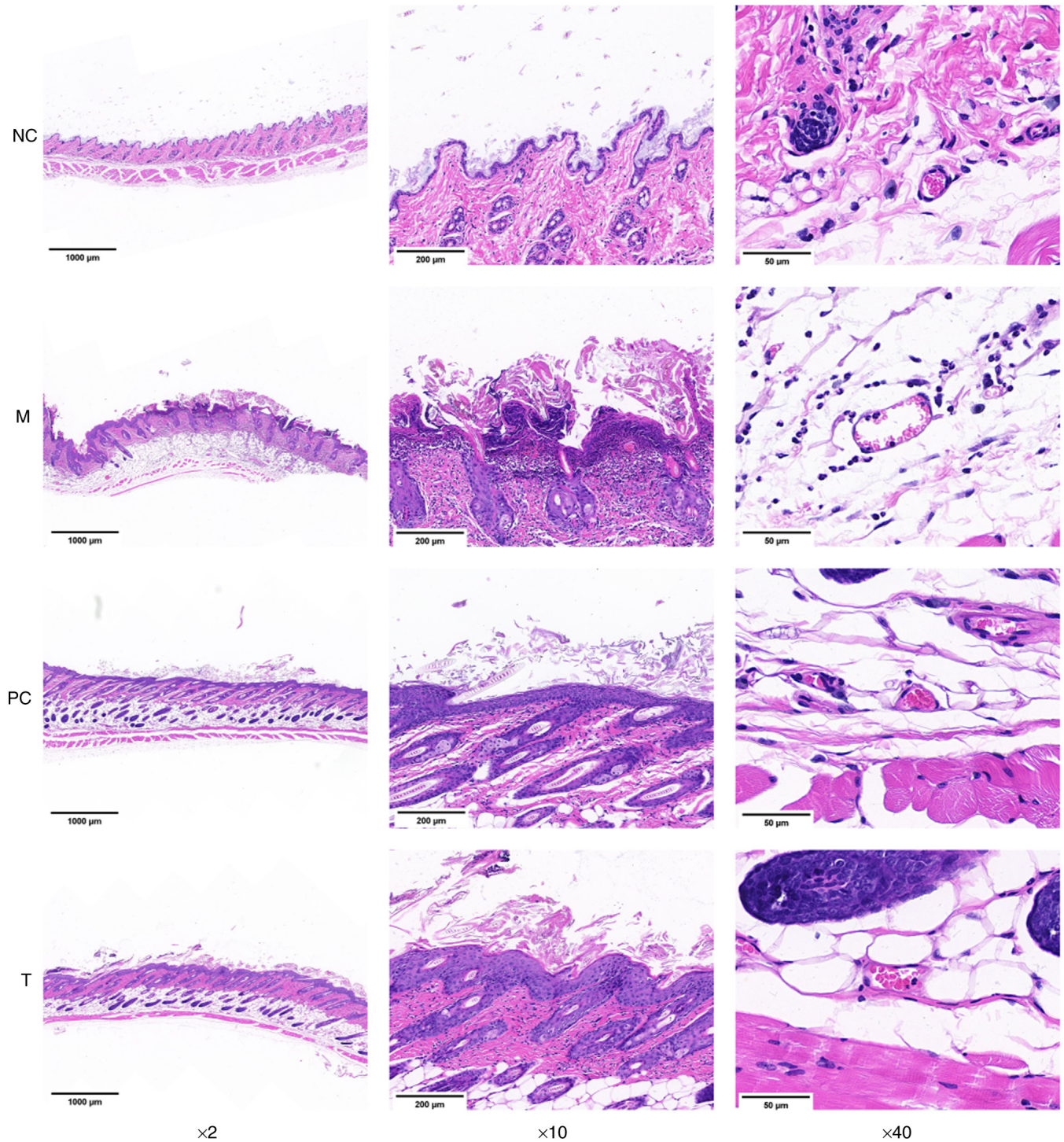

Figure 1. Representative microscopic manifestations of H&E staining of skin tissues in each group (n=6 per group). Magnification, x2, x10 and x40. M, trichloroethylene model; PC, positive control; T, TNF-α antagonist treatment; NC, vehicle control.

specificity. All reactions were performed in triplicate with Cq standard deviation <0.3. The primer sequences used were as follows: RORγt forward: 5'-GACCCACACCTCACAAATTGA-3' and reverse: 5'-AGTAGGCCACATTACACTGCT-3'; Foxp3 forward: 5'-CCCAGGAAAGACAGCAACCTT-3' and reverse: 5'-TTCTCACAACCAGGCCACTTG-3'; and GAPDH (loading control) forward: 5'-AGGTCGGTGTGAACGGATTTG-3' and reverse: 5'-TGTAGACCATGTAGTTGAGGTCA-3'. Relative expression was determined using the $2^{-\Delta\Delta Cq}$ method normalized to GAPDH (36).

Statistical analysis. All experimental data are expressed as the mean ± SD. Statistical analyses were performed using GraphPad Prism (version 9.0; Dotmatics). Comparisons among multiple groups were conducted using one-way ANOVA tests, with inter-group comparisons analyzed by Tukey's post hoc tests. Correlation analyses were performed using Pearson's correlation coefficient. Sample size calculations were performed based on preliminary data, with n=6 providing 80% power to detect a 40% difference at α=0.05. P<0.05 was considered to indicate a statistically significant difference.

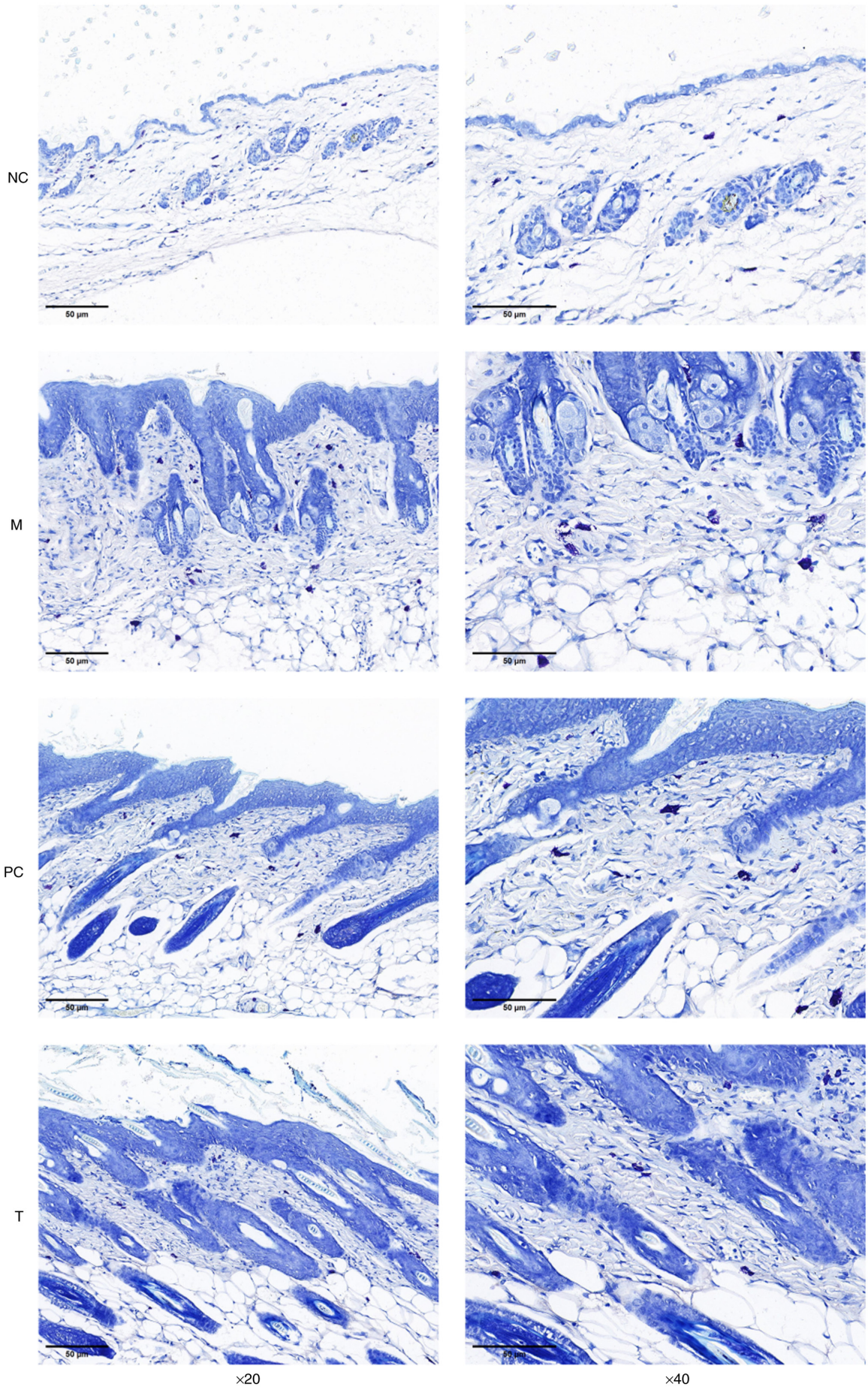

Figure 2. Toluidine blue staining results of samples from different treatment groups (n=6 per group). Scale bars, 50 μm. M, trichloroethylene model; PC, positive control; T, TNF-α antagonist treatment; NC, vehicle control.

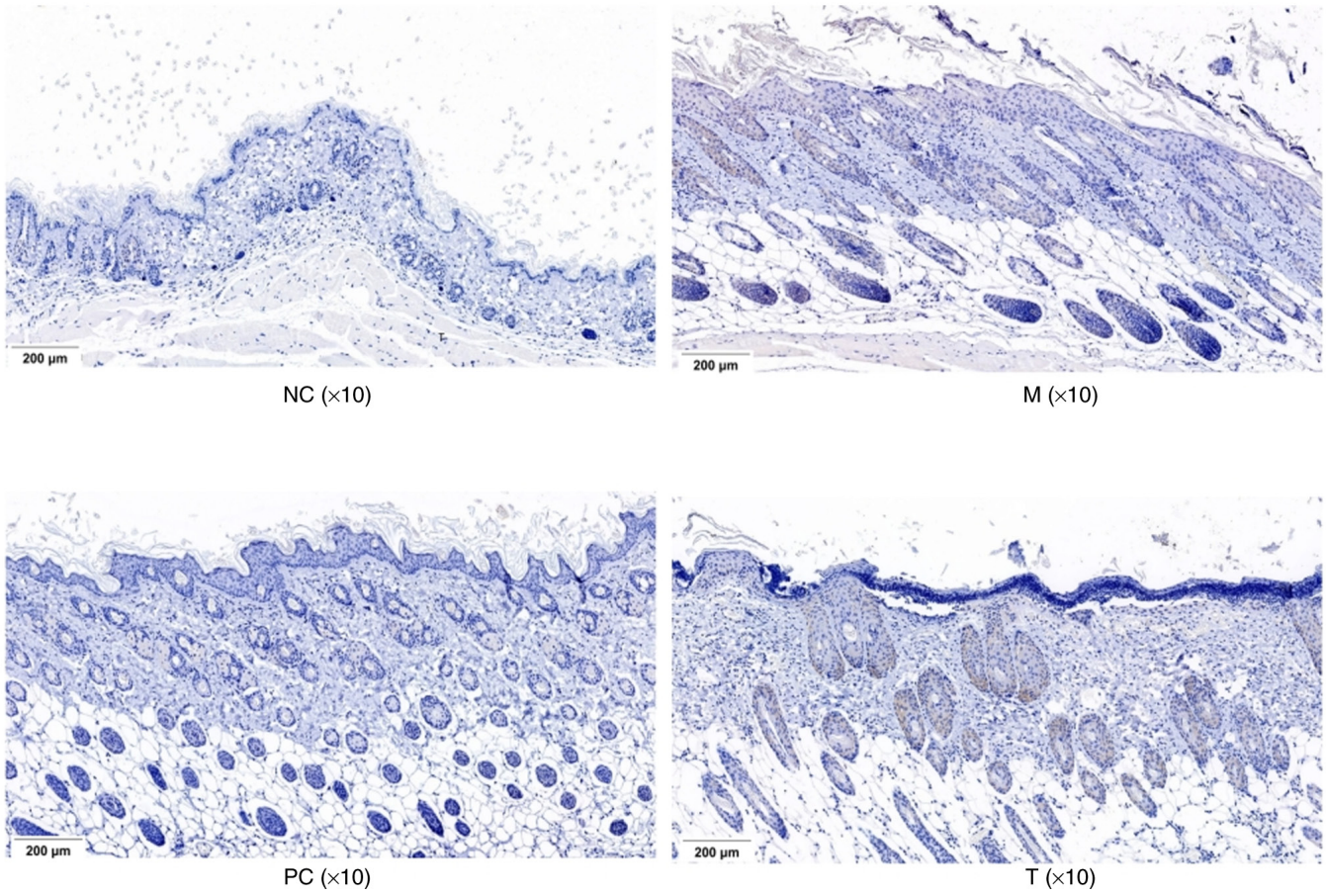

Figure 3. Caspase-3 expression in skin tissues from each experimental group (n=6 per group). Scale bars, 200 μm. NC, vehicle control; M, trichloroethylene model; PC, positive control; T, TNF-α antagonist treatment.

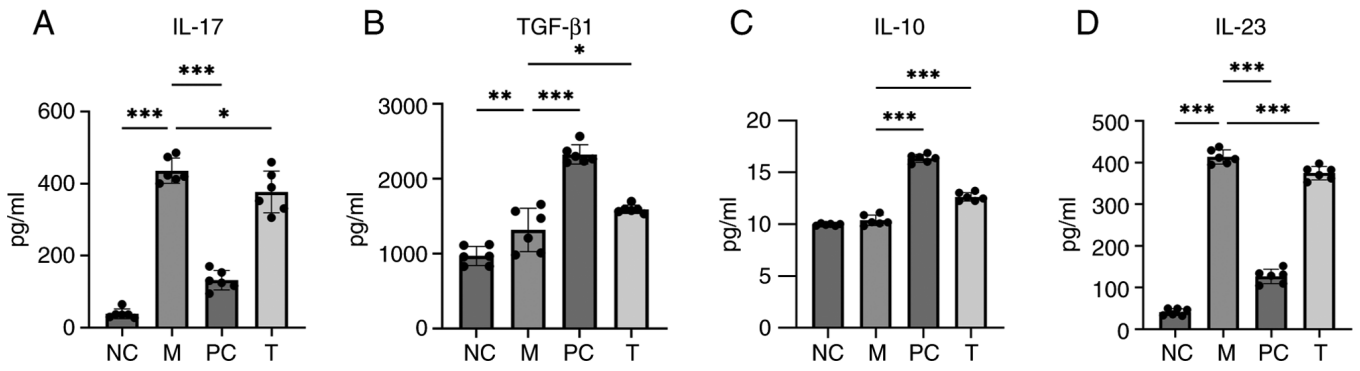

Figure 4. Comparison of serum (A) IL-17, (B) TGF-β1, (C) IL-10 and (D) IL-23 levels in each group. Data are presented as the mean ± SD (n=6 per group). Statistical significance was determined by one-way ANOVA with Tukey's post hoc test. *P<0.05, **P<0.01 and ***P<0.001. NC, vehicle control; M, trichloroethylene model; PC, positive control; T, TNF-α antagonist treatment.

Results

TNF-α inhibition improves histopathological features. H&E staining revealed that TCE exposure induced extensive epidermal necrosis, architectural disarray and dense dermal leukocyte infiltration in the M group (Fig. 1). Both PC and T treatments markedly attenuated these pathological changes, with the protective effects of TNF-α blockade comparable to those of conventional corticosteroid therapy (37).

TNF-α blockade normalizes mast cell distribution. Toluidine blue staining showed that TCE exposure caused pronounced cytomorphological alterations and heterogeneous mast cell distribution in the M group (Fig. 2). TNF-α antagonist administration markedly normalized mast cell presentation and distribution patterns, indicating effective reversal of TCE-induced mast cell dysregulation.

Caspase-3 overexpression coincides with Th17/Treg imbalance. Immunohistochemistry analysis revealed that the M group

Table I. Summary of experimental data across all groups.

Group	IL-17	TGF-β1	IL-10	IL-23	Tregs	Th17	Foxp3	RORγt
NC	38.40±13.50	967.99±127.57	9.97±0.11	41.00±8.27	13.05±0.64	3.11±0.61	1.00±0.08	1.00±0.05
M	435.90±35.09[a]	1,315.50±290.44	10.38±0.51	413.33±17.04[a]	5.58±1.46[a]	11.64±1.93[a]	0.15±0.02[a]	4.66±0.51[a]
PC	131.59±26.89[a,b]	2,323.56±129.79[a,b]	16.35±0.39[a,b]	126.47±17.21[a,b]	11.7±0.36[b,c]	4.57±0.38[b,c]	0.84±0.08[b,c]	1.78±0.25[b,c]
T	377.02±58.23[a]	1,591.49±56.50[a]	12.64±0.41[a,b]	374.47±16.32[a,b]	8.85±0.88[a,b]	7.92±1.32[a,b]	0.53±0.07[a,b]	2.24±0.34[a,b]

[a]P<0.01, [b]P<0.01 vs. M group and [c]P<0.05 vs. NC group. n=6 per group. NC, vehicle control; M, trichloroethylene model; PC, positive control; T, TNF-α antagonist treatment; RORγt, retinoic acid-related orphan receptor γ-t; Tregs, regulatory T cells; Th17, T helper 17.

exhibited a significantly higher level of Caspase-3-positive cells compared with the control group, indicating elevated apoptosis in the local tissue microenvironment (Fig. 3). Flow cytometric analysis further demonstrated an increased proportion of Th17 cells and a decreased proportion of Treg cells in the M group. Notably, the elevated Caspase-3 expression coincided with reduced Treg frequencies, suggesting that enhanced apoptosis may contribute to Treg loss. By contrast, despite the increased apoptotic signal, the Th17 population was expanded, implying that Th17 cell activation and differentiation outweigh apoptosis under these conditions. Treatment with the TNF-α inhibitor markedly decreased Caspase-3-positive staining, restored the Th17/Treg balance, and alleviated tissue inflammation.

TNF-α antagonist restores systemic cytokine balance. Serum cytokine quantification revealed that IL-17 and IL-23 levels were significantly elevated in the M group (435.90±35.09 pg/ml and 413.33±17.04 pg/ml, respectively) compared with the NC group (38.40±13.50 pg/ml and 41.00±8.27 pg/ml), representing 11.4- and 10.1-fold increases, respectively (both P<0.01; Fig. 4; Table I). Moderate increases in IL-10 and TGF-β1 were also observed. Both therapeutic interventions significantly reduced IL-17 and IL-23 levels (P<0.01 vs. M), with TNF-α blockade decreasing IL-17 to 377.02±58.23 pg/ml (a 13.5% reduction) and IL-23 to 374.47±16.32 pg/ml (a 9.4% reduction), while maintaining elevated regulatory cytokines, demonstrating restoration of immune homeostasis.

Treg frequency is restored by TNF-α blockade. Flow cytometry demonstrated a significant reduction in Treg cell proportion in the M group (5.58±1.46%) compared with NC (13.05±0.64%), representing a 57.2% decrease (P<0.01). Both TNF-α antagonist and methylprednisolone treatments significantly reversed this reduction (P<0.001 vs. M), restoring Treg frequencies to 8.85±0.88% (2.27-fold increase) and 11.7±0.36% (2.10-fold increase), respectively, to levels comparable with NC (Fig. 5A; Table I). Representative dot plots showed the proportions of $CD4^+CD25^+Foxp3^+$ Treg cells within the $CD4^+$ gate were 12.4% in NC, 4.57% in M, 11.2% in PC and 8.82% in T group, demonstrating significant Treg reduction following TCE exposure and partial restoration after TNF-α antagonist treatment (Fig. 5B).

Th17 expansion is attenuated by TNF-α antagonist treatment. Proportion of Th17 cells was significantly increased in the M group (11.64±1.93%) relative to the NC group (3.11±0.61%), representing a 3.74-fold increase (P<0.01), consistent with elevated serum IL-17 levels. TNF-α antagonist treatment reduced Th17 cell frequencies to 7.92±1.32% (32.0% reduction vs. M; P<0.01), indicating partial normalization rather than complete correction, as levels remained elevated compared with NC (3.11±0.61%) and the PC group (4.57±0.38%; Fig. 6A; Table I). Representative dot plots showed the proportions of $CD4^+IL\text{-}17A^+$ Th17 cells within the $CD4^+$ gate were 2.16% in NC, 12.5% in M, 4.88% in PC and 7.62% in T group, demonstrating marked Th17 expansion after TCE exposure and partial attenuation by TNF-α antagonist treatment (Fig. 6B).

Magnetic bead sorting yields high-purity $CD3^+$ T cells. Flow cytometric analysis showed that the proportion of $CD3^+$ T

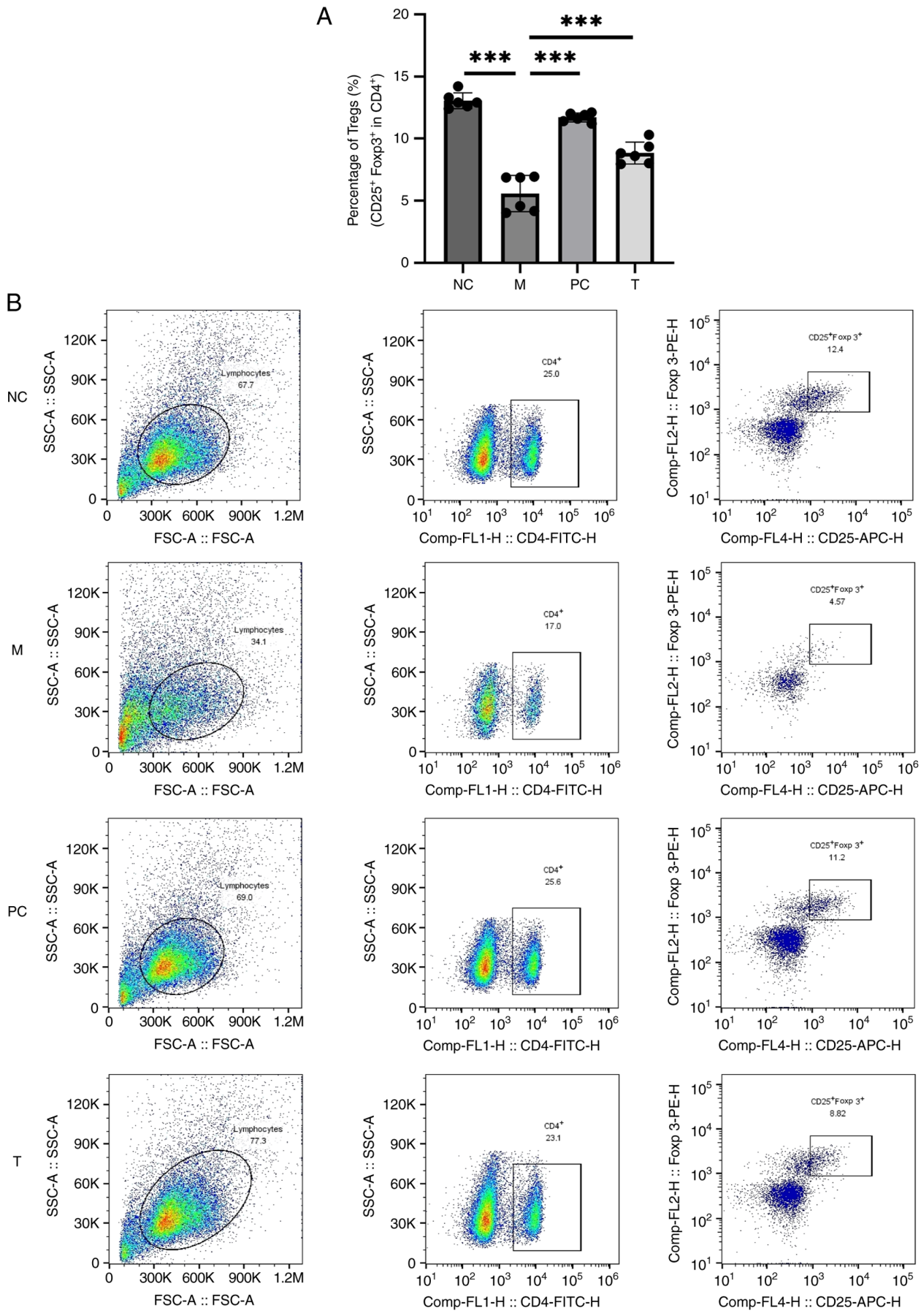

Figure 5. (A) Comparison of the proportion of Tregs in peripheral blood of each group. (B) Representative flow cytometry plots of Tregs in the peripheral blood of each group. Data are presented as the means ± SD (n=6 per group). Statistical significance was determined by one-way ANOVA with Tukey's post hoc test. ***P<0.001. Tregs, regulatory T cells; NC, vehicle control; M, trichloroethylene model; PC, positive control; T, TNF-α antagonist treatment; SSC-A, side scatter area; FSC-A, forward scatter area.

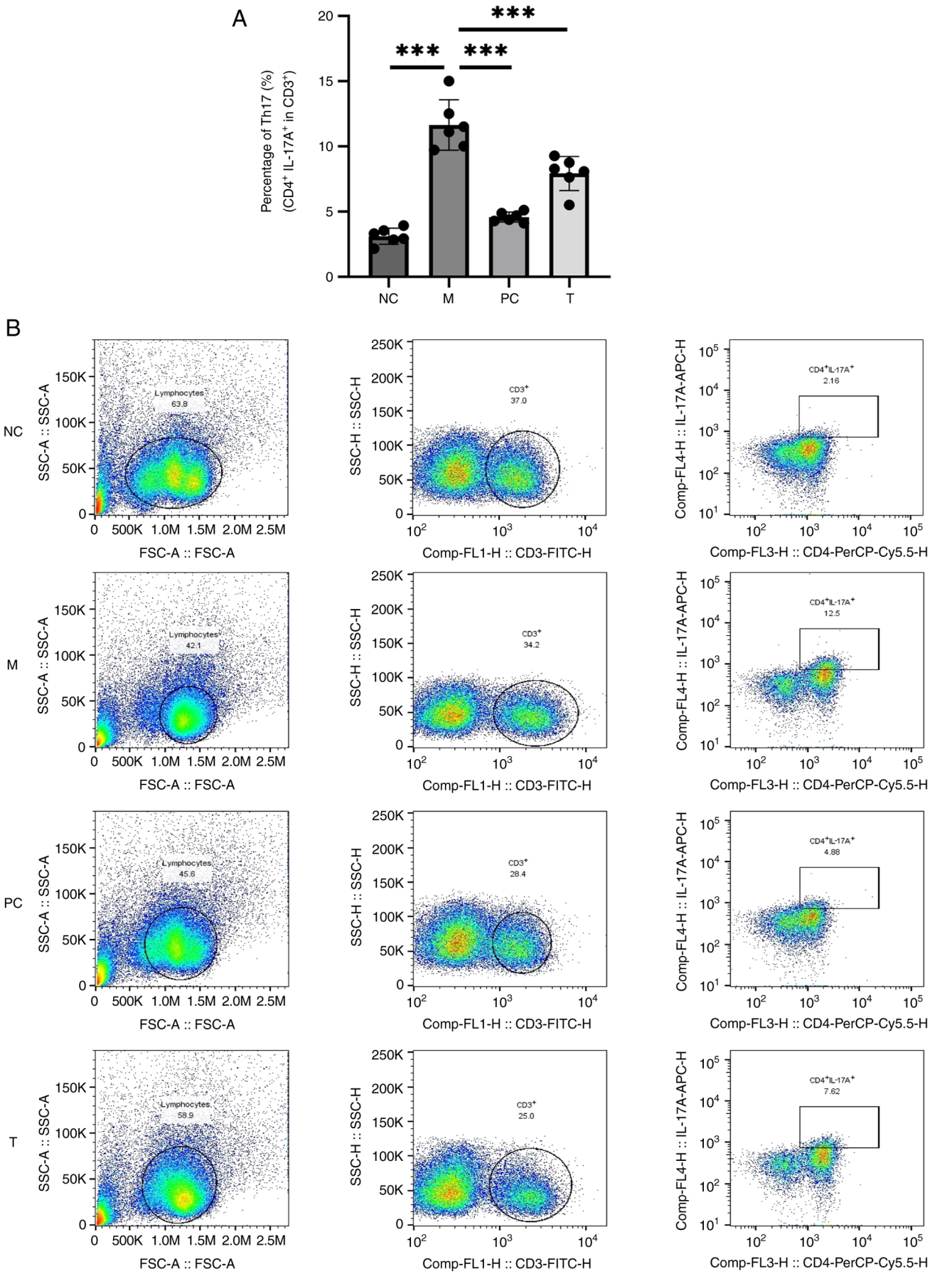

Figure 6. (A) Proportion of Th17 cells in the peripheral blood of each group. (B) Representative flow cytometry plots of Th17 cells in the peripheral blood of each group. Data are presented as the means ± SD (n=6 per group). Statistical significance was determined by one-way ANOVA with Tukey's post hoc test. ***P<0.001. Th17, T helper 17; NC, vehicle control; M, trichloroethylene model; PC, positive control; T, TNF-α antagonist treatment; SSC-A, side scatter area; FSC-A, forward scatter area.

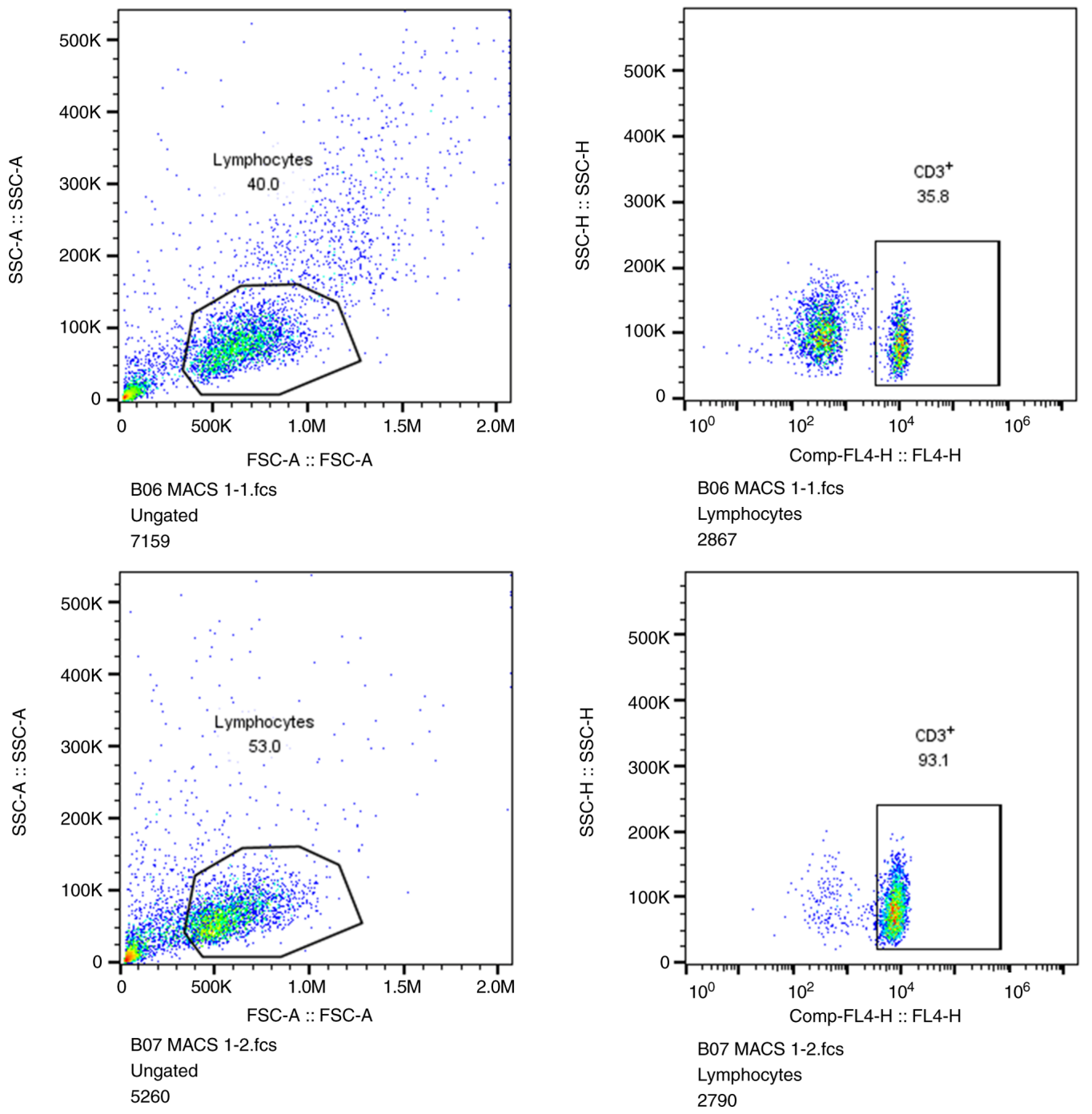

Figure 7. Flow cytometry analysis of the proportion of CD3+ T cells before and after magnetic bead sorting (n=6 per group). SSC-A, side scatter area; FSC-A, forward scatter area.

cells increased from 53.0% in pre-sorted PBMCs to 93.1% in post-sorted populations, determining high-purity CD3+ T cell isolation (>95%) suitable for subsequent qPCR analysis (Fig. 7).

TNF-α blockade reverses RORγt/Foxp3 transcriptional imbalance. RT-qPCR analysis of purified CD3+ T cells revealed that RORγt mRNA expression was significantly upregulated in the M group (4.66±0.51 fold-change) compared with the NC group (1.00±0.05), representing a 4.66-fold increase (P<0.01), while Foxp3 mRNA expression was markedly downregulated (0.15±0.02 fold-change) compared with the NC group (1.00±0.08), representing an 85% reduction (P<0.01; Fig. 8; Table I). TNF-α antagonist treatment significantly suppressed RORγt expression to 2.24±0.34 fold-change (52.0% reduction vs. M; P<0.01) and elevated Foxp3 expression to 0.53±0.07 fold-change (3.5-fold increase vs. M; P<0.01), restoring both transcriptional factors to levels not significantly different from NC.

Discussion

Within the present study, a key development in understanding the immunopathogenesis of SJS/TEN was established by

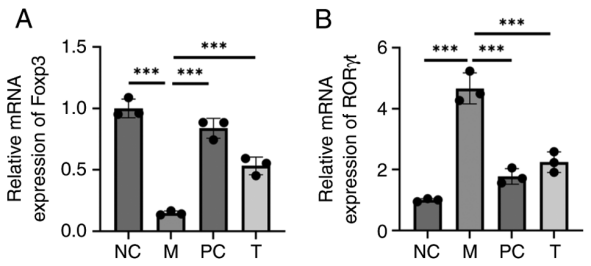

Figure 8. mRNA expression levels of (A) RORγt and (B) Foxp3 in purified CD3+ T cells measured by reverse transcription-quantitative PCR. Data are presented as the mean ± SD (n=6 per group). Statistical significance was determined by one-way ANOVA with Tukey's post hoc test. ***P<0.001. NC, vehicle control; M, trichloroethylene model; PC, positive control; T, TNF-α antagonist treatment; RORγt, retinoic acid-related orphan receptor γ-t.

demonstrating that disease progression is driven by disruption of the Th17/Treg balance through dysregulation of the RORγt/Foxp3 transcriptional axis. The present findings revealed that TNF-α blockade restored this immune equilibrium, providing a novel mechanistic explanation for its therapeutic efficacy, distinguishing the present study from previous descriptive clinical reports (11,38,39).

The central innovation of this research lies in connecting specific transcriptional regulation within CD3+ T cells to clinical pathology through controlled experimental evidence. While prior clinical studies have noted altered Th17/Treg ratios in patients with SJS/TEN (38,40-42), the present study uniquely demonstrated the causative role of RORγt/Foxp3 dysregulation in driving this imbalance and established TNF-α blockade as a targeted corrective intervention. This represents a notable conceptual advancement beyond existing literature that primarily describes cytokine profiles without elucidating upstream regulatory mechanisms (3,23).

The present study made three distinctive contributions to the field: First, providing experimental validation of the 'immunological imbalance hypothesis' in SJS/TEN pathogenesis through controlled animal studies, offering stronger causal evidence compared with previous observational human studies (43,44); second, identifying the RORγt/Foxp3 axis as a specific molecular target for therapeutic intervention, moving beyond broad immunosuppressive approaches (28,45); and third, revealing that TNF-α blockade functions through immunomodulation rather than simple anti-inflammatory action, explaining its improved efficacy in a number of refractory cases compared with conventional treatments (46-48).

Compared with related studies investigating corticosteroid or IVIG therapies that broadly suppress immune responses (49,50), the present findings suggest a more targeted approach focused on rebalancing specific T cell subsets. This represents a paradigm shift from non-specific immunosuppression toward precision immunomodulation in SJS/TEN management. The therapeutic mechanism identified in the present study, namely simultaneous suppression of RORγt and restoration of Foxp3, differs from the broad-spectrum effects of conventional treatments, potentially explaining variable clinical responses observed in practice, including inconsistent effects on mortality reduction and heterogeneous outcomes across different patient populations (47,48).

The present study advances the field by providing a mechanistic framework that bridges clinical observations with molecular immunology (19,25). The demonstration that TNF-α blockade can improve clinical outcomes in SJS/TEN, with evidence suggesting immunomodulatory effects on T cell responses, extends current understanding of its mode of action and supports its strategic use in SJS/TEN management (46,47). Furthermore, the present findings suggested that monitoring Th17/Treg ratios and RORγt/Foxp3 expression could provide predictive biomarkers for treatment response, addressing a marked clinical need for personalized therapeutic strategies (23,28).

Beyond the established Th17/Treg imbalance, the present histopathological findings revealed marked mast cell accumulation and degranulation in TCE-exposed skin lesions, which were markedly attenuated by TNF-α blockade. Mast cells are increasingly recognized as key effectors in severe cutaneous adverse reactions, capable of releasing pro-inflammatory mediators including TNF-α, IL-17 and proteases that exacerbate tissue damage (51,52). Notably, mast cell-T cell cross-talk has been shown to potentiate Th17 polarization and sustain local inflammation (53). The present study therefore proposes that mast cell infiltration contributes to the inflammatory milieu that reinforces RORγt-driven Th17 differentiation, creating a positive feedback loop that amplifies skin injury. The observed reduction in mast cell density following TNF-α antagonist treatment suggests that its therapeutic effects extend beyond direct T cell modulation to include interruption of mast cell-driven inflammatory cascades, likely by neutralizing pre-formed TNF-α stored in mast cell granules and suppressing mast cell-dependent cytokine amplification loops (54,55). These findings position mast cells as both contributors to SJS/TEN pathology and potential ancillary targets for therapeutic intervention.

The observed shifts in Th17 and Treg frequencies call into question whether they result from altered differentiation, survival or trafficking of T cells. The present transcriptional data, particularly the reciprocal changes in RORγt and Foxp3 mRNA expression, suggest that altered lineage commitment is a primary mechanism. The 4.66-fold upregulation of RORγt and the 85% reduction of Foxp3 in CD3+ T cells suggest the transcriptional reprogramming favored Th17 polarization at the expense of Treg development. These findings were consistent with studies showing that RORγt and Foxp3 antagonistically regulate CD4+ T cell differentiation (39,56). However, it should be acknowledged that the present data cannot fully exclude contributions from enhanced apoptosis of Tregs or preferential recruitment of Th17 cells to inflamed skin. Indeed, reduced Treg proportions may also reflect increased susceptibility to activation-induced cell death in the highly inflammatory microenvironment (57), while elevated tissue homing receptors (such as C-C chemokine receptor types 4 and 6) on Th17 cells could promote their accumulation in lesions (58). Future studies incorporating Ki-67 proliferation assays, Annexin V apoptosis staining and analysis of chemokine receptor expression profiles are warranted to further investigate the relative contributions of differentiation, survival and trafficking to the Th17/Treg imbalance in SJS/TEN.

A number of limitations should be acknowledged. First, while the present murine model provided valuable mechanistic

insights, it could not fully replicate the complex genetic and pharmacological factors involved in human SJS/TEN (22,59). Second, the sample size (n=6 per group) was relatively modest, which may have limited the statistical power of detecting smaller effect sizes; however, it was sufficient to demonstrate significant differences in primary outcomes based on preliminary power calculation. Third, only male mice were used in the present study to minimize hormonal variability, but this introduced a sex bias; future studies should aim to include female cohorts to assess potential sex-dependent differences in disease pathogenesis and treatment response. Fourth, it should be acknowledged that infliximab, a chimeric monoclonal antibody targeting human TNF-α, exhibits limited cross-reactivity with murine TNF-α (60). To address this potential limitation, the dosage and administration regimen employed in the present study were carefully selected based on prior reports demonstrating functional efficacy of infliximab in murine inflammatory models (61,62). In addition, the observed therapeutic effects, including significant suppression of RORγt expression, restoration of Foxp3 levels and rebalancing of the Th17/Treg ratio, provide functional validation of its biological activity in the present experimental context. Despite this, it should be acknowledged that the use of species-specific anti-murine TNF-α antibodies (such as etanercept or anti-mouse TNF-α monoclonal antibody) would be more pharmacologically appropriate for future mechanistic studies. Fifth, while significant changes in Treg proportions were observed, functional suppression assays to directly assess Treg suppressive capacity were not performed. Such assays (including *in vitro* co-culture suppression tests) would provide more definitive evidence for Treg dysfunction in SJS/TEN and its restoration by TNF-α blockade and should be incorporated in future investigations. Finally, the focus on $CD4^+$ T cells, while revealing important mechanisms, does not exclude potential contributions from other immune cell populations, including cytotoxic $CD8^+$ T cells and γδ T cells, which warrant further investigation (11,63).

The present study recommends that future research should: i) Validate the present findings in clinical cohorts through prospective biomarker studies (23,28); ii) investigate the interaction between TNF-α blockade and other immunomodulatory therapies to optimize combination strategies (48,64); iii) explore the potential of targeting the RORγt/Foxp3 axis with more specific pharmacological agents (14,17); and iv) examine genetic polymorphisms that might influence individual responses to TNF-α blockade in patients with SJS/TEN (22,65).

In conclusion, the present study demonstrated that SJS/TEN pathogenesis involves dysregulation of the RORγt/Foxp3 transcriptional axis, leading to severe Th17/Treg imbalance. In the TCE-exposed model group, the Th17/Treg ratio increased to 2.10±0.68 from 0.24±0.05 in normal controls. Molecular analysis further demonstrated this imbalance, showing a 4.66-fold upregulation of RORγt mRNA and a reduction of Foxp3 mRNA to only 15% of control levels in $CD3^+$ T cells. This cellular dysregulation was accompanied by a pronounced inflammatory response. Serum levels of IL-17 and IL-23 increased to 435.90±35.09 pg/ml and 413.33±17.04 pg/ml respectively, ~11.4-fold and 10.1-fold increases over control levels. IL-10 levels also increased, with the highest level observed in the PC group (16.35±0.39 pg/ml). TNF-α blockade effectively corrected these pathological changes. Treatment restored the Th17/Treg ratio to 0.90±0.19, suppressed RORγt expression by 52% (2.24±0.34 fold-change) and elevated Foxp3 expression by 3.5-fold (0.53±0.07 fold-change). Inflammatory cytokines showed partial reductions, with IL-17 and IL-23 decreasing to 377.02±58.23 pg/ml and 374.47±16.32 pg/ml respectively, while IL-10 levels remained elevated at 12.64±0.41 pg/ml. These integrated findings provide evidence that TNF-α blockade ameliorates SJS/TEN by restoring immune homeostasis through transcriptional reprogramming of the RORγt/Foxp3 axis, downregulating RORγt expression while upregulating Foxp3 expression, thereby rebalancing the Th17/Treg equilibrium. The present data establish a clear mechanistic rationale for TNF-α-targeted therapy and identified potential biomarkers for monitoring therapeutic response.

Acknowledgements

Not applicable.

Funding

The present study was supported by The Public Welfare Scientific Research Guidance Projects in The Field of Agriculture and Social Development of China (grant no. 20241029Y033).

Availability of data and materials

The data generated in the present study may be requested from the corresponding author.

Authors' contributions

ZM wrote the manuscript. WZ and SFX conducted the experiments. TTS designed the present study. ZM and WZ analyzed and interpreted the data. XCX contributed to data analysis and interpretation. TTS and XCX confirm the authenticity of all the raw data. All authors have read and approved the final manuscript.

Ethics approval and consent to participate

The present animal study was reviewed and approved by The Lab of Animal Experimental Ethical Inspection of Zhejiang Deruikang Biotechnology Co., Ltd. (approval no. DRK-20250301281).

Patient consent for publication

Not applicable.

Competing interests

The authors declare that they have no competing interests.

References

1. Charlton OA, Harris V, Phan K, Mewton E, Jackson C and Cooper A: Toxic epidermal necrolysis and Steven-Johnson syndrome: A comprehensive review. Adv Wound Care (New Rochelle) 9: 426-439, 2020.

2. Mockenhaupt M: Stevens-Johnson syndrome and toxic epidermal necrolysis: Clinical patterns, diagnostic considerations, etiology, and therapeutic management. Semin Cutan Med Surg 33: 10-16, 2014.
3. Duong TA, Valeyrie-Allanore L, Wolkenstein P and Chosidow O: Severe cutaneous adverse reactions to drugs. Lancet 390: 1996-2011, 2017.
4. Oakley AM and Krishnamurthy K: Stevens-Johnson syndrome. StatPearls. Treasure Island (FL): StatPearls Publishing Copyright © 2026, StatPearls Publishing LLC., 2026.
5. Zahra FT, Imtiaz A, Khan A and Fatima M: JAK inhibitors in toxic epidermal necrolysis a new frontier in therapeutics. Ann Med Surg (Lond) 88: 1206-1208, 2026.
6. Murphy TJ, Fijany AJ, Swafford EP, Garcia JT, Vyas P, Beyene RT, Gondek SP, Wagner AL, Patel MB and Slater ED: The outcomes of SJS/TEN: A nationwide analysis. J Burn Care Res: irag010, 2026 (Epub ahead of print).
7. Schneider JA and Cohen PR: Stevens-Johnson syndrome and toxic epidermal necrolysis: A concise review with a comprehensive summary of therapeutic interventions emphasizing supportive measures. Adv Ther 34: 1235-1244, 2017.
8. Creamer D, Walsh SA, Dziewulski P, Exton LS, Lee HY, Dart JKG, Setterfield J, Bunker CB, Ardern-Jones MR, Watson KMT, *et al*: UK guidelines for the management of Stevens-Johnson syndrome/toxic epidermal necrolysis in adults 2016. J Plast Reconstr Aesthet Surg 69: e119-e153, 2016.
9. Yamane Y, Matsukura S, Watanabe Y, Yamaguchi Y, Nakamura K, Kambara T, Ikezawa Z and Aihara M: Retrospective analysis of Stevens-Johnson syndrome and toxic epidermal necrolysis in 87 Japanese patients-treatment and outcome. Allergol Int 65: 74-81, 2016.
10. Zimmermann S, Sekula P, Venhoff M, Motschall E, Knaus J, Schumacher M and Mockenhaupt M: Systemic immunomodulating therapies for Stevens-Johnson syndrome and toxic epidermal necrolysis: A systematic review and meta-analysis. JAMA Dermatol 153: 514-522, 2017.
11. Chung WH, Hung SI, Yang JY, Su SC, Huang SP, Wei CY, Chin SW, Chiou CC, Chu SC, Ho HC, *et al*: Granulysin is a key mediator for disseminated keratinocyte death in Stevens-Johnson syndrome and toxic epidermal necrolysis. Nat Med 14: 1343-1350, 2008.
12. Chung WH, Hung SI, Hong HS, Hsih MS, Yang LC, Ho HC, Wu JY and Chen YT: Medical genetics: A marker for Stevens-Johnson syndrome. Nature 428: 486, 2004.
13. White KD, Abe R, Ardern-Jones M, Beachkofsky T, Bouchard C, Carleton B, Chodosh J, Cibotti R, Davis R, Denny JC, *et al*: SJS/TEN 2017: Building multidisciplinary networks to drive science and translation. J Allergy Clin Immunol Pract 6: 38-69, 2018.
14. Ivanov II, McKenzie BS, Zhou L, Tadokoro CE, Lepelley A, Lafaille JJ, Cua DJ and Littman DR: The orphan nuclear receptor RORgammat directs the differentiation program of proinflammatory IL-17+ T helper cells. Cell 126: 1121-1133, 2006.
15. Harrington LE, Hatton RD, Mangan PR, Turner H, Murphy TL, Murphy KM and Weaver CT: Interleukin 17-producing CD4+ effector T cells develop via a lineage distinct from the T helper type 1 and 2 lineages. Nat Immunol 6: 1123-1132, 2005.
16. Zhu J and Paul WE: CD4 T cells: Fates, functions, and faults. Blood 112: 1557-1569, 2008.
17. Hori S, Nomura T and Sakaguchi S: Control of regulatory T cell development by the transcription factor Foxp3. Science 299: 1057-1061, 2003.
18. Brunkow ME, Jeffery EW, Hjerrild KA, Paeper B, Clark LB, Yasayko SA, Wilkinson JE, Galas D, Ziegler SF and Ramsdell F: Disruption of a new forkhead/winged-helix protein, scurfin, results in the fatal lymphoproliferative disorder of the scurfy mouse. Nat Genet 27: 68-73, 2001.
19. Noack M and Miossec P: Th17 and regulatory T cell balance in autoimmune and inflammatory diseases. Autoimmun Rev 13: 668-677, 2014.
20. Lee GR: The balance of Th17 versus treg cells in autoimmunity. Int J Mol Sci 19: 730, 2018.
21. Nistala K and Wedderburn LR: Th17 and regulatory T cells: Rebalancing pro- and anti-inflammatory forces in autoimmune arthritis. Rheumatology (Oxford) 48: 602-606, 2009.
22. Tapia B, Padial A, Sánchez-Sabaté E, Alvarez-Ferreira J, Morel E, Blanca M and Bellón T: Involvement of CCL27-CCR10 interactions in drug-induced cutaneous reactions. J Allergy Clin Immunol 114: 335-340, 2004.
23. Stern RS and Divito SJ: Stevens-Johnson syndrome and toxic epidermal necrolysis: Associations, outcomes, and pathobiology-thirty years of progress but still much to be done. J Invest Dermatol 137: 1004-1008, 2017.
24. Tohyama M, Watanabe H, Murakami S, Shirakata Y, Sayama K, Iijima M and Hashimoto K: Possible involvement of CD14+ CD16+ monocyte lineage cells in the epidermal damage of Stevens-Johnson syndrome and toxic epidermal necrolysis. Br J Dermatol 166: 322-330, 2012.
25. Paquet P and Piérard GE: Soluble fractions of tumor necrosis factor-alpha, interleukin-6 and of their receptors in toxic epidermal necrolysis: A comparison with second-degree burns. Int J Mol Med 1: 459-462, 1998.
26. Nassif A, Bensussan A, Dorothée G, Mami-Chouaib F, Bachot N, Bagot M, Boumsell L and Roujeau JC: Drug specific cytotoxic T-cells in the skin lesions of a patient with toxic epidermal necrolysis. J Invest Dermatol 118: 728-733, 2002.
27. Schwartz RA, McDonough PH and Lee BW: Toxic epidermal necrolysis: Part II. Prognosis, sequelae, diagnosis, differential diagnosis, prevention, and treatment. J Am Acad Dermatol 69: 187.e1-e16, 203-204, 2013.
28. Tian CC, Ai XC, Ma JC, Hu FQ, Liu XT, Luo YJ, Tan GZ, Zhang JM, Li XQ, Guo Q, *et al*: Etanercept treatment of Stevens-Johnson syndrome and toxic epidermal necrolysis. Ann Allergy Asthma Immunol 129: 360-365.e1, 2022.
29. Cao J, Zhang X, Xing X and Fan J: Biologic TNF-α inhibitors for Stevens-Johnson syndrome, toxic epidermal necrolysis, and TEN-SJS overlap: A study-level and patient-level meta-analysis. Dermatol Ther (Heidelb) 13: 1305-1327, 2023.
30. Wang H, Zhang JX, Li SL, Wang F, Zha WS, Shen T, Wu C and Zhu QX: An animal model of trichloroethylene-induced skin sensitization in BALB/c mice. Int J Toxicol 34: 442-453, 2015.
31. Azukizawa H: Animal models of toxic epidermal necrolysis. J Dermatol 38: 255-260, 2011.
32. Böyum A: Isolation of mononuclear cells and granulocytes from human blood. Isolation of monuclear cells by one centrifugation, and of granulocytes by combining centrifugation and sedimentation at 1 g. Scand J Clin Lab Invest Suppl 97: 77-89, 1968.
33. Enerbäck L: Mast cells in rat gastrointestinal mucosa. 2. Dye-binding and metachromatic properties. Acta Pathol Microbiol Scand 66: 303-312, 1966.
34. Ramos-Vara JA: Technical aspects of immunohistochemistry. Vet Pathol 42: 405-426, 2005.
35. Annunziato F, Cosmi L, Santarlasci V, Maggi L, Liotta F, Mazzinghi B, Parente E, Filì L, Ferri S, Frosali F, *et al*: Phenotypic and functional features of human Th17 cells. J Exp Med 204: 1849-1861, 2007.
36. Livak KJ and Schmittgen TD: Analysis of relative gene expression data using real-time quantitative PCR and the 2(-Delta Delta C(T)) method. Methods 25: 402-408, 2001.
37. Wang CW, Yang LY, Chen CB, Ho HC, Hung SI, Yang CH, Chang CJ, Su SC, Hui RCY, Chin SW, *et al*: Randomized, controlled trial of TNF-α antagonist in CTL-mediated severe cutaneous adverse reactions. J Clin Invest 128: 985-996, 2018.
38. Teraki Y, Kawabe M and Izaki S: Possible role of TH17 cells in the pathogenesis of Stevens-Johnson syndrome and toxic epidermal necrolysis. J Allergy Clin Immunol 131: 907-909, 2013.
39. Zhou L, Lopes JE, Chong MMW, Ivanov II, Min R, Victora GD, Shen Y, Du J, Rubtsov YP, Rudensky AY, *et al*: TGF-beta-induced Foxp3 inhibits T(H)17 cell differentiation by antagonizing RORgammat function. Nature 453: 236-240, 2008.
40. Ueta M, Kannabiran C, Wakamatsu TH, Kim MK, Yoon KC, Seo KY, Joo CK, Sangwan V, Rathi V, Basu S, *et al*: Trans-ethnic study confirmed independent associations of HLA-A*02:06 and HLA-B*44:03 with cold medicine-related Stevens-Johnson syndrome with severe ocular surface complications. Sci Rep 4: 5981, 2014.
41. Ushigome Y, Mizukawa Y, Kimishima M, Yamazaki Y, Takahashi R, Kano Y and Shiohara T: Monocytes are involved in the balance between regulatory T cells and Th17 cells in severe drug eruptions. Clin Exp Allergy 48: 1453-1463, 2018.
42. Sun L, Zhao Q, Ao S, Liu T, Wang Z, You J, Mi Z, Sun Y, Xue X, Ogese MO, *et al*: Feedback regulation of VISTA and Treg by TNF-α controls T cell responses in drug allergy. Allergy 80: 1400-1416, 2025.
43. Hama N, Aoki S, Chen CB, Hasegawa A, Ogawa Y, Vocanson M, Asada H, Chu CY, Lan CCE, Dodiuk-Gad RP, *et al*: Recent progress in Stevens-Johnson syndrome/toxic epidermal necrolysis: Diagnostic criteria, pathogenesis and treatment. Br J Dermatol 192: 9-18, 2024.

44. Chen CB, Abe R, Pan RY, Wang CW, Hung SI, Tsai YG and Chung WH: An updated review of the molecular mechanisms in drug hypersensitivity. J Immunol Res 2018: 6431694, 2018.
45. Milojevic D, Nguyen KD, Wara D and Mellins ED: Regulatory T cells and their role in rheumatic diseases: A potential target for novel therapeutic development. Pediatr Rheumatol Online J 6: 20, 2008.
46. Zhang S, Tang S, Li S, Pan Y and Ding Y: Biologic TNF-alpha inhibitors in the treatment of Stevens-Johnson syndrome and toxic epidermal necrolysis: A systemic review. J Dermatolog Treat 31: 66-73, 2020.
47. Heuer R, Paulmann M, Mockenhaupt M and Nast A: Systemic immunomodulating therapies for epidermal necrolysis (Stevens-Johnson syndrome/toxic epidermal necrolysis): A systematic review and meta-analysis. J Dtsch Dermatol Ges 24: 34-42, 2026.
48. Umemura M, Okamoto-Yoshida Y, Yahagi A, Touyama S, Nakae S, Iwakura Y and Matsuzaki G: Involvement of IL-17A-producing TCR γδ T cells in late protective immunity against pulmonary Mycobacterium tuberculosis infection. Immun Inflamm Dis 4: 401-412, 2016.
49. Roujeau JC: The spectrum of Stevens-Johnson syndrome and toxic epidermal necrolysis: A clinical classification. J Invest Dermatol 102: 28S-30S, 1994.
50. Roujeau JC: Treatment of severe drug eruptions. J Dermatol 26: 718-722, 1999.
51. Yao L, Baltatzis S, Zafirakis P, Livir-Rallatos C, Voudouri A, Markomichelakis N, Zhao T and Foster CS: Human mast cell subtypes in conjunctiva of patients with atopic keratoconjunctivitis, ocular cicatricial pemphigoid and Stevens-Johnson syndrome. Ocul Immunol Inflamm 11: 211-222, 2003.
52. Yu X, Kasprick A, Hartmann K and Petersen F: The role of mast cells in autoimmune bullous dermatoses. Front Immunol 9: 386, 2018.
53. Suurmond J, van Heemst J, van Heiningen J, Dorjée AL, Schilham MW, van der Beek FB, Huizinga TW, Schuerwegh AJM and Toes REM: Communication between human mast cells and CD4(+) T cells through antigen-dependent interactions. Eur J Immunol 43: 1758-1768, 2013.
54. Chatterjea D, Paredes L, Martinov T, Balsells E, Allen J, Sykes A and Ashbaugh A: TNF-alpha neutralizing antibody blocks thermal sensitivity induced by compound 48/80-provoked mast cell degranulation. F1000Res 2: 178, 2013.
55. Wershil BK, Furuta GT, Lavigne JA, Choudhury AR, Wang ZS and Galli SJ: Dexamethasone or cyclosporin A suppress mast cell-leukocyte cytokine cascades. Multiple mechanisms of inhibition of IgE- and mast cell-dependent cutaneous inflammation in the mouse. J Immunol 154: 1391-1398, 1995.
56. Yang XO, Pappu BP, Nurieva R, Akimzhanov A, Kang HS, Chung Y, Ma L, Shah B, Panopoulos AD, Schluns KS, *et al*: T helper 17 lineage differentiation is programmed by orphan nuclear receptors ROR alpha and ROR gamma. Immunity 28: 29-39, 2008.
57. Pandiyan P, Zheng L, Ishihara S, Reed J and Lenardo MJ: CD4+CD25+Foxp3+ regulatory T cells induce cytokine deprivation-mediated apoptosis of effector CD4+ T cells. Nat Immunol 8: 1353-1362, 2007.
58. Acosta-Rodriguez EV, Rivino L, Geginat J, Jarrossay D, Gattorno M, Lanzavecchia A, Sallusto F and Napolitani G: Surface phenotype and antigenic specificity of human interleukin 17-producing T helper memory cells. Nat Immunol 8: 639-646, 2007.
59. Hung SI, Mockenhaupt M, Blumenthal KG, Abe R, Ueta M, Ingen-Housz-Oro S, Phillips EJ and Chung WH: Severe cutaneous adverse reactions. Nat Rev Dis Primers 10: 30, 2024.
60. Irani Y, Scotney P, Nash A and Williams KA: Species cross-reactivity of antibodies used to treat ophthalmic conditions. Invest Ophthalmol Vis Sci 57: 586-591, 2016.
61. Shen C, Maerten P, Geboes K, Van Assche G, Rutgeerts P and Ceuppens JL: Infliximab induces apoptosis of monocytes and T lymphocytes in a human-mouse chimeric model. Clin Immunol 115: 250-259, 2005.
62. Lopetuso LR, Petito V, Cufino V, Arena V, Stigliano E, Gerardi V, Gaetani E, Poscia A, Amato A, Cammarota G, *et al*: Locally injected Infliximab ameliorates murine DSS colitis: Differences in serum and intestinal levels of drug between healthy and colitic mice. Dig Liver Dis 45: 1017-1021, 2013.
63. Gibson A, Ram R, Gangula R, Li Y, Mukherjee E, Palubinsky AM, Campbell CN, Thorne M, Konvinse KC, Choshi P, *et al*: Multiomic single-cell sequencing defines tissue-specific responses in Stevens-Johnson syndrome and toxic epidermal necrolysis. Nat Commun 15: 8722, 2024.
64. Zhou L, Lu Y, Zou Y, Wei H, Guo X, Li Q, Zhou Y, Zhao X, Xie F and Zhang L: Drug-induced Stevens-Johnson syndrome and toxic epidermal necrolysis: A 10-year retrospective study of 103 cases. Clin Exp Dermatol 50: 2200-2208, 2025.
65. Chung WH, Chang WC, Lee YS, Wu YY, Yang CH, Ho HC, Chen MJ, Lin JY, Hui RC, Ho JC, *et al*: Genetic variants associated with phenytoin-related severe cutaneous adverse reactions. JAMA 312: 525-534, 2014.